
DEPARTMENT OF STATISTICS

The University of Wisconsin
Madison, Wisconsin

TECHNICAL REPORT NO. 287

November 1971

AN ITERATIVE METHOD TO APPROXIMATE
THE SOLUTION OF A FREDHOLM INTEGRAL
EQUATION OF THE FIRST KIND

By

Bernard L. Viort

Typist: Jacquelyn R. Jones

This research was supported by the National Science Foundation
under grant GA-18908, and by the Wisconsin Alumni Research
Foundation.

AN ITERATIVE METHOD TO APPROXIMATE THE SOLUTION OF A FREDHOLM
INTEGRAL EQUATION OF THE FIRST KIND

by Bernard L. Viort

Department of Statistics

I. Summary.

A method is presented to find an approximate numerical solution of the Fredholm integral equation of the first kind. The method is a modification of the procedure initiated by CHAHINE [1] and extended by SMITH [2]:

- Spline functions are introduced in order to reduce consistently the computing time and to increase the flexibility of application,
- Acceleration parameters are introduced in order to improve the empirical rate of convergence.

II. The problem.

Given the measurements: μ_i^0 , $i=1, \dots, n$ and the kernel: $K(x, y)$, $K(x, y) \geq 0$ find a function $f^0(x)$ such that

$$\mu_i^0 = \int K(x, y_i) f^0(x) dx \quad (1)$$

where the y_i , $i=1, \dots, n$ are also given.

It is well known that the solution of this problem is not unique and many different methods have been proposed to find a solution restricted to a given space of functions.

This type of problem appears in different fields like:

- In meteorological remote sensing where $f^0(x)$ represents an unknown temperature or humidity profile as a function of altitude and $K(x,y)$ is a kernel representing the spectral transmissivity gradient.
- In studies of light scattered from small particle suspensions where $f^0(x)$ represents an unknown particle size density as a function of particle radius and $K(X,y)$ is a kernel derived from Mie theory.
- In statistics, where the Wiener-Hopf integral equation corresponds to the special form of kernel: $K(x,y) = K(x-y)$.
- More generally in situations where the measurements are linear functions of an unknown distribution.

III. 1. Chahine's Method.

Chahine based his algorithm on the following idea: Let $f^{(1)}(x)$ be a first approximation of $f^0(x)$, and consider the corresponding

$$\mu_i^1 = \int K(x, y_i) f^1(x) dx \quad (i=1, \dots, n) \quad (2)$$

In order to get exactly μ_i^0 , one solution is to consider the function

$$\frac{\mu_i^0}{\mu_i} f^1(x) \quad (3)$$

and the same remark is valid for all $i=1, \dots, n$. Since the modified function $(\mu_i^0/\mu_i) f^1(x)$ appears with the kernel function $K(x, y_i)$, Chahine suggests the use of this function when $K(x, y_i)$ is relatively important with respect to the $K(x, y_j)$, ($j=1, \dots, n$; $j \neq i$) in the following way:

$$f^2(x) = \begin{cases} \sum_{i=1}^n f^1(x) \frac{\mu_i^0}{\mu_i} \frac{K(x, y_i)}{\sum_{j=1}^n K(x, y_j)} & \text{for } \sum_{j=1}^n K(x, y_j) \neq 0 \\ \frac{1}{n} \sum_{i=1}^n f^1(x) \frac{\mu_i^0}{\mu_i} & \text{for } \sum_{j=1}^n K(x, y_j) = 0 \end{cases} \quad (4)$$

the iterative formula being then

$$f^N(x) = f^{N-1}(x) \sum_{i=1}^n \frac{\mu_i^0}{\mu_i^{N-1}} \frac{K(x, y_i)}{\sum_{j=1}^n K(x, y_j)} \quad (5)$$

where:

$$\mu_i^{N-1} = \int K(x, y_i) f^{N-1}(x) dx \quad (6)$$

III. 2. Remarks on the convergence of Chahine's method.

The convergence of the method is not mentioned in the original article: it seems to be a difficult problem since the method is nonlinear.

However there is the relationship:

$$\sum_{i=1}^n \mu_i^N = \sum_{i=1}^n \mu_i^0 \quad (7)$$

which means that if $(n-1)$ of the μ_i^N converge to the corresponding μ_i^0 , then the last μ_i^N converge also to the corresponding μ_i^0 , as $N \rightarrow \infty$.

Proof:

$$\sum_{i=1}^n \mu_i^N = \sum_{i=1}^n \int K(x, y_i) f^N(x) dx \quad (8)$$

$$= \int f^{N-1}(x) \sum_{i=1}^n \left[K(x, y_i) \sum_{j=1}^n \frac{\mu_j^0}{\mu_j^{N-1}} \frac{K(x, y_j)}{\sum_{k=1}^n K(x, y_k)} \right] dx \quad (9)$$

$$= \int f^{N-1}(x) \sum_{j=1}^n \frac{\mu_j^0}{\mu_j^{N-1}} K(x, y_j) dx \quad (10)$$

$$= \sum_{j=1}^n \mu_j^0 \quad (11)$$

since

$$\mu_j^{N-1} = \int K(x, y_j) f^{N-1}(x) dx \quad (12)$$

More generally, if instead of the sum $\sum_{i=1}^n K(x, y_i)$ we consider

a linear combination $\sum_{i=1}^n \lambda_i K(x, y_i)$, $\lambda_i \geq 0$, $i=1, \dots, n$ there is the relationship:

$$\sum_{i=1}^n \lambda_i \mu_{\lambda_i}^N = \sum_{i=1}^n \lambda_i \mu_i^0 \quad (13)$$

where

$$\mu_{\lambda_i}^N = \int K(x, y_i) f^N(x) dx \quad (14)$$

and

$$f_{\lambda}^N(x) = f_{\lambda}^{N-1}(x) \sum_{i=1}^n \frac{\mu_i^0}{\mu_{\lambda_i}^{N-1}} \frac{K(x, y_i)}{\sum_{j=1}^n \lambda_j K(x, y_j)} \quad (15)$$

III. 3. Computational aspects.

Since it is necessary to compute n integrals of the form

$$\int K(x, y_i) f^{N-1}(x) dx \quad (16)$$

for each iteration, with sufficient accuracy, the application of the method turns out to be very expensive.

IV. Introduction of cubic splines.

The spline functions, (Schoenberg [3], Greville [4]), are of frequent use in approximation theory. The underlying assumption is that the unknown function $f^0(x)$ can be well approximated by piecewise polynomials, given its values at the points (often called "knots") x_0, \dots, x_m .

Without entering into the details, let just give the example of the cubic spline:

given the knots x_0, \dots, x_m
and the values $f^0(x_0), \dots, f^0(x_m)$

the cubic spline of approximation will be the function

$$\begin{aligned} \tilde{f}(x) &= a_{0i} + a_{1i}x + a_{2i}x^2 + a_{3i}x^3 \quad * \\ &\text{for } x \in [x_{i-1}, x_i] \\ &\quad i=1, \dots, m \end{aligned} \quad (17)$$

where the coefficients $a_{ki}, k=0, \dots, 3$

$i=1, \dots, m$

are uniquely determined by the following conditions:

$$\begin{aligned} S_1: \quad \tilde{f}(x_i) &= f^0(x_i) \quad i=0, \dots, m \\ S_2: \quad \tilde{f}'(x) \text{ and } \tilde{f}''(x) &\text{ are continuous functions of } x \\ S_3: \quad \tilde{f}'''(x_0) &= \tilde{f}'''(x_m) = 0 \end{aligned}$$

The first condition means that \tilde{f} is an approximation of f^0 , since they take the same values at the points where f^0 is known.

* Note: or equivalently

$$\begin{aligned} \tilde{f}(x) &= \alpha_{0i} + \alpha_{1i}(x-x_{i-1}) + \alpha_{2i}(x-x_{i-1})^2 + \alpha_{3i}(x-x_{i-1})^3 \quad (17') \\ &\text{for } x \in [x_{i-1}, x_i] \end{aligned}$$

form leading to more accurate numerical results in the following.

The second condition means that \tilde{f} is a smooth function over the whole range of x , since its first two derivatives are continuous.

The third condition, necessary to grant uniqueness, has a less appealing meaning.

Intuitively one can think that, if the function to be approximated is smooth enough (continuous and not too oscillating) the spline approximation with a sufficient but reasonable number of knots is a very good one. In order to illustrate this point, two examples are given in Figure 1.

Returning to our problem, the advantages of this modification are related to:

- The economy of computing time, the quantities

$$\mu_i^N = \int_{x_0}^{x_m} K(x, y_i) f^N(x) dx \quad N=0, 1, \dots \quad (18)$$

can be approximated by

$$\mu_i^N = \int_{x_0}^{x_m} K(x, y_i) \tilde{f}^N(x) dx \quad (19)$$

when \tilde{f}^N is an approximation of f^N , and (19) turn out to be

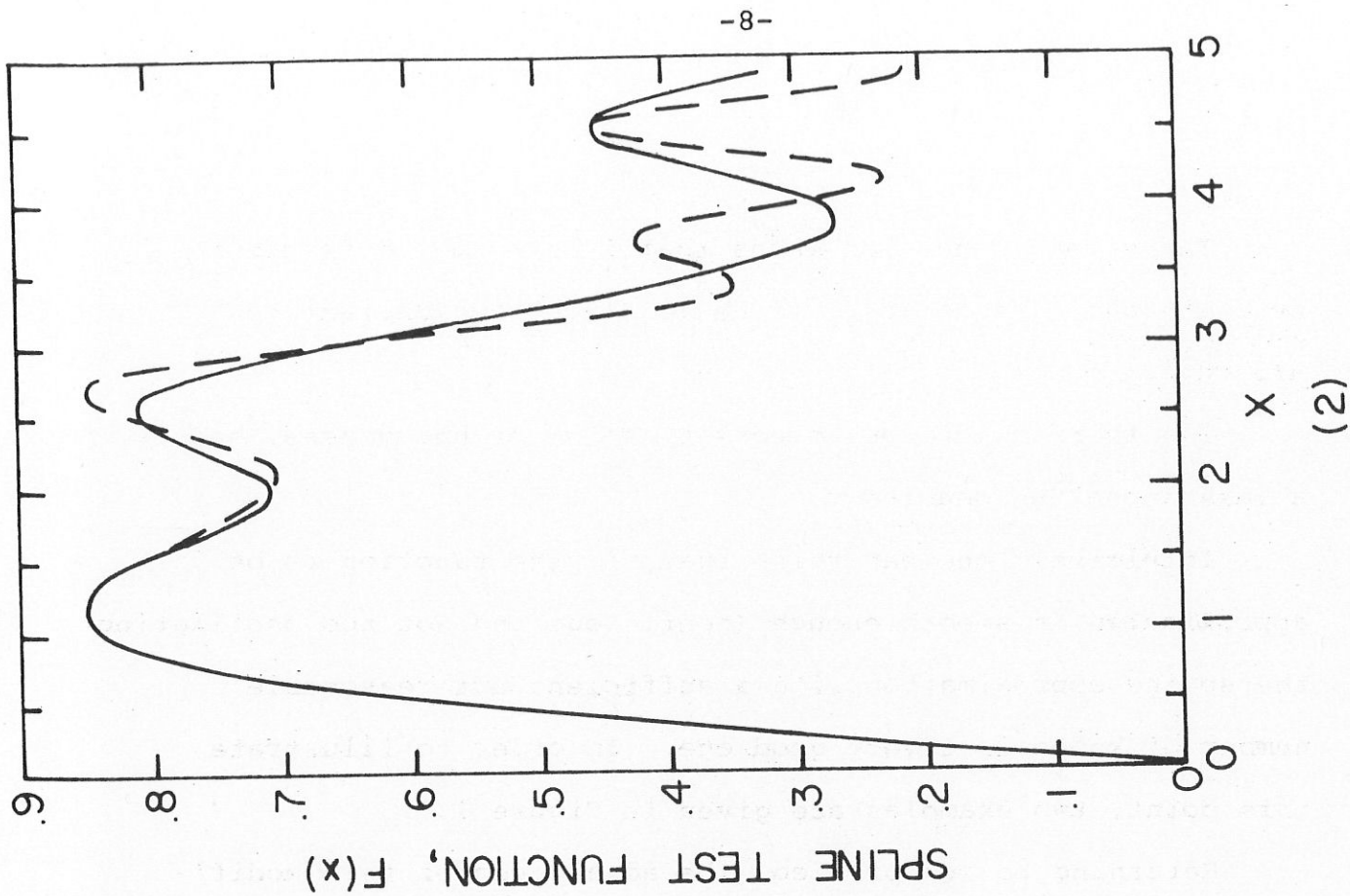
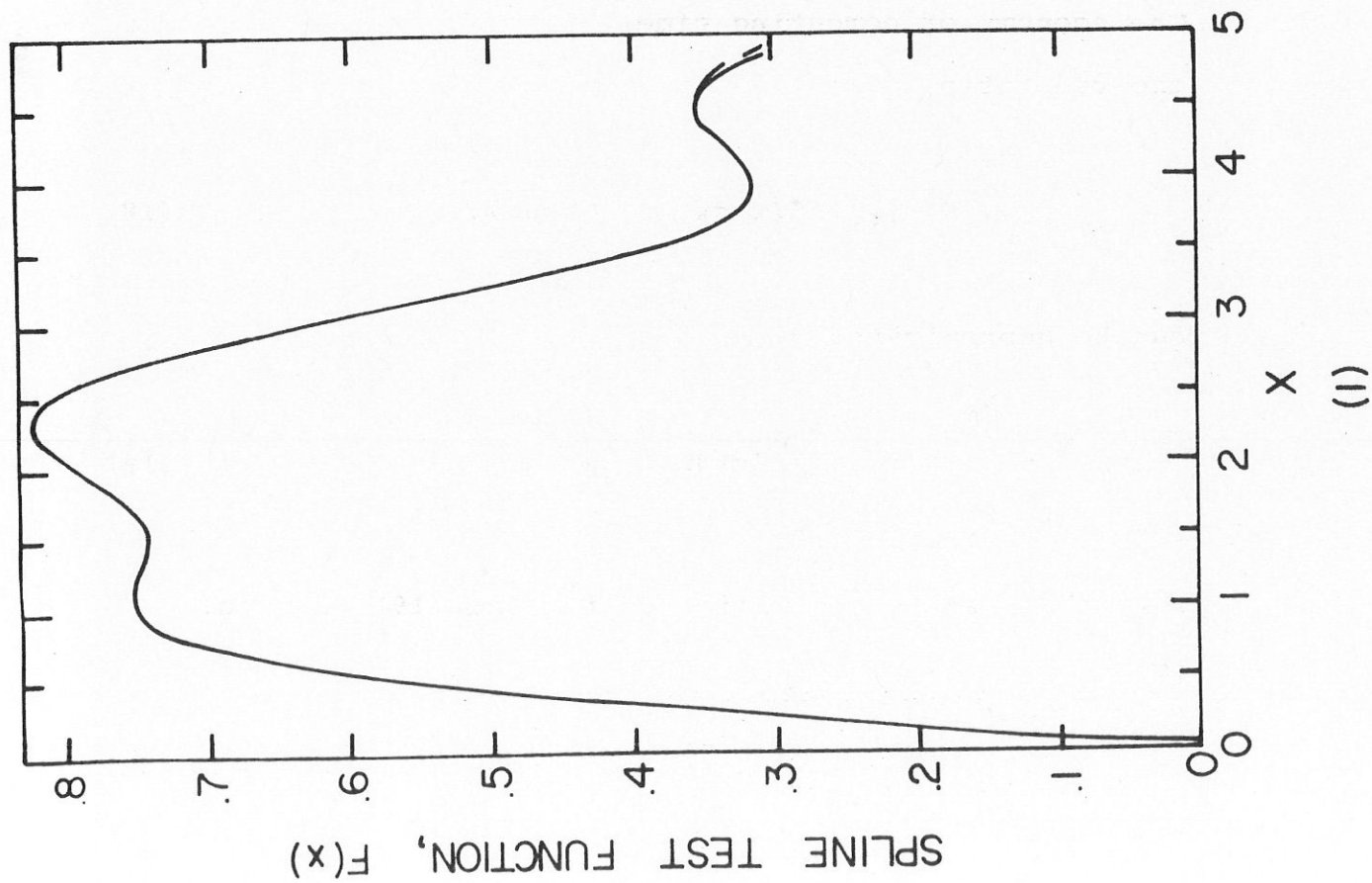


Figure 1. Examples of spline approximations to two functions, $F(x)$.
Actual function, — — —. Spline approximation, —.

$$\tilde{u}_i^N = \sum_{k=1}^m \sum_{a=0}^3 \alpha_{ak}^N \int_{x_{k-1}}^{x_k} K(x, y_i) (x - x_{k-1})^a dx \quad (20)$$

this means that the quantities

$$\int_{x_{k-1}}^{x_k} K(x, y_i) (x - x_{k-1})^a dx \quad (21)$$

$i=1, \dots, n$
 $k=1, \dots, m$
 $a=0, \dots, 3$

are computed once and for all with great accuracy, and then stored for future use.

- The flexibility of function handling.

A smooth function is then represented by $m+1$ values

$$f(x_0), \dots, f(x_m)$$

instead of an analytical form. This is of great interest when it is desired to vary the shape of the different functions (unknown distribution $f^0(x)$ as well as first approximation $f^1(x)$)

A possible disadvantage appears clearly when considering the discretized iteration formula:

$$\tilde{f}^N(x_k) = \tilde{f}^{N-1}(x_k) \sum_{i=1}^n \frac{\tilde{u}_i^0}{\tilde{u}_i^{N-1}} \frac{K(x_k, y_i)}{\sum_{j=1}^n K(x_k, y_j)} \quad (22)$$

namely the fact that the influence of the different kernels $K(x, y_i)$ can be systematically biased by an unfortunate choice of the knots x_k : the use of spline approximation introduces

a new dimension to the problem of optimal design.

However, the present approximation reduced the computing time by roughly a factor of 100 as compared with Chahine's algorithm. The examples presented in the following section were therefore all derived with splines.

V. Two improvements of the method of Chahine and Smith.

V. I. Normalization.

The method using the relative value of the kernels, it therefore seems sensible to introduce some kind of normalization in order to give a comparable importance to all the kernels: if one of the $K(x, y_i)$ is always greater than the others, for instance, it should not mean that it is more important as would be implied by

$$\frac{K(x, y_i)}{\sum_{j=1}^n K(x, y_j)} \quad (23)$$

since $K(x, y) \geq 0$, the kernels were modified in such a way that

$$\int K^*(x, y_i) dx = 1 \quad i=1, \dots, n \quad (24)$$

$$\text{i.e.} \quad K^*(x, y_i) = \frac{K(x, y_i)}{\int K(x, y_i) dx} \quad i=1, \dots, n \quad (25)$$

It is to be noted that this is not the only possible normalization, and one can use for instance

$$\left[\int [K^*(x,y)]^2 dx \right]^{\frac{1}{2}} = 1 \quad (26)$$

V. 2. Introduction of acceleration parameters.

Since the rate of convergence depends on the ratios

$$\left[\frac{\tilde{\mu}_i^0}{\tilde{\mu}_i^N} \right] \quad \text{the convergence may be accelerated by the use of}$$

$$\left[\frac{\tilde{\mu}_i^0}{\tilde{\mu}_i^N} \right]^{\alpha} \quad \alpha > 1 \quad (27)$$

when all the ratios approach 1.

A first strategy was used that consists in starting with $\alpha=1$ and then changing to $\alpha=2$ after a fixed number of iteration.

A second strategy was to start with $\alpha=1$ and to change α for α' , where

$$\alpha' = p / \max_i \left| \frac{\tilde{\mu}_i^0}{\tilde{\mu}_i^N} - 1 \right| \quad 0 < p < 1 \quad (28)$$

as soon as:

$$\max_i \left| \frac{\tilde{\mu}_i^0}{\tilde{\mu}_i^N} - 1 \right| < p \quad 0 < p < 1$$

so that, in each case:

$$\text{either} \quad \max_i \left| \left[\frac{\tilde{\mu}_i^0}{\tilde{\mu}_i^N} \right]^{\alpha'} \right| \approx 1 + p \quad (29)$$

$$\text{or} \quad \min_i \left| \left[\frac{\tilde{\mu}_i^0}{\tilde{\mu}_i^N} \right]^{\alpha} \right| \approx 1 - p \quad (30)$$

VI. Numerical Results.

All the curves presented in Appendix II correspond to the same kernel

$$K(x,y) = \{ \sin(xy)/xy - \cos(xy) \}^2 \quad (31)$$

which is an approximation of a diffraction kernel used in atmospheric physic for small angles (for more details see Appendix I). Due to the origin of the kernel, the variable y will in the following be referred as "angle" or "angle of observation" since it corresponds to the angle between the direction of the source of light under study and the axis of the instrucment of measure.

Figure 2.a represents the general shape of $K(x,y)$, which is more or less "stretched" along the x -axis according to the value of y .

It is to be noted that this kernel does not correspond to a favorable situation, since the functions $K(x,y_i)$ are not

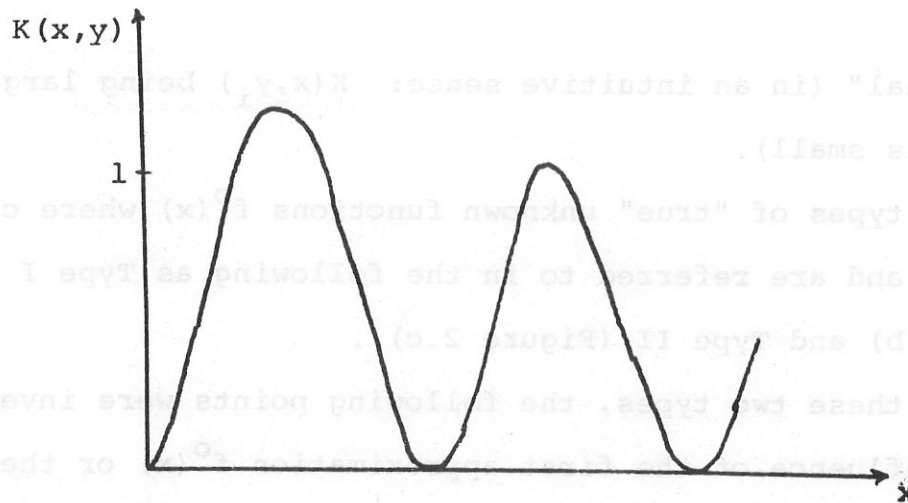


Figure 2.a. $K(x,y)$ as a function of x for fixed y .

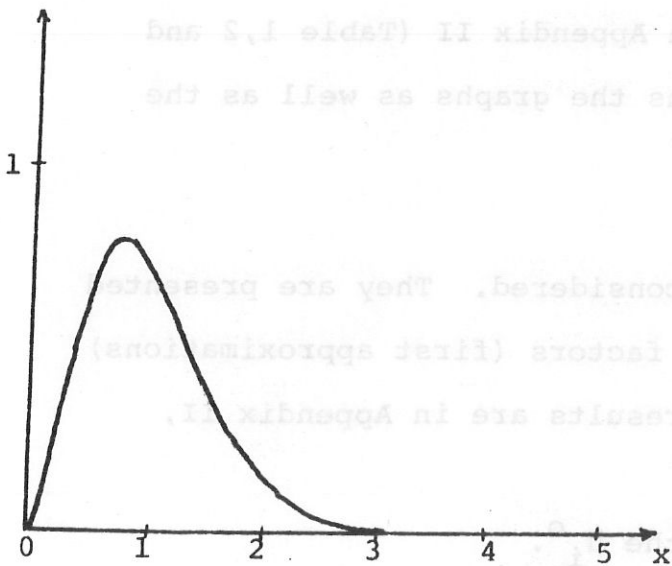


Figure 2.b. Type I "true" $f^0(x)$.

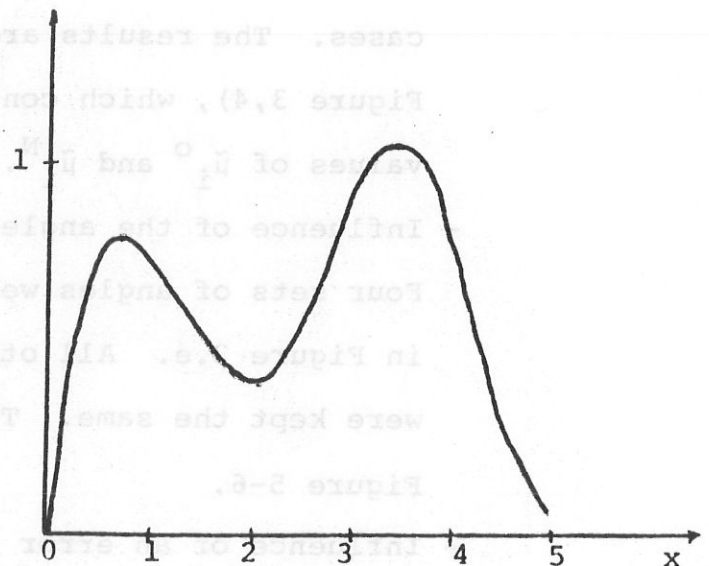


Figure 2.c. Type II "true" $f^0(x)$.

"orthogonal" (in an intuitive sense: $K(x, y_i)$ being large when $K(x, y_j)$ is small).

Two types of "true" unknown functions $f^0(x)$ were considered, and are referred to in the following as Type I (see Figure 2.b) and Type II (Figure 2.c) .

For these two types, the following points were investigated:

- Influence of the first approximation $f^0(x)$ or the solution. Four different first approximations were considered, and are shown in Figure 2.d.

In order to make a comparison, all other factors (angles, number of iteration,...) were the same in all cases. The results are in Appendix II (Table 1,2 and Figure 3,4), which contains the graphs as well as the values of $\tilde{\mu}_i^0$ and $\tilde{\mu}_i^N$.

- Influence of the angles.

Four sets of angles were considered. They are presented in Figure 2.e. All other factors (first approximations) were kept the same. The results are in Appendix II, Figure 5-6.

- Influence of an error on the $\tilde{\mu}_i^0$.

A gaussian noise was introduced, such that

$$\tilde{\mu}_i^{0'} = \tilde{\mu}_i^0 + \epsilon_i \quad (32)$$

where ϵ_i are Normal independent variables, with mean 0 and standard deviation proportional to the value of $\tilde{\mu}_i^0$.

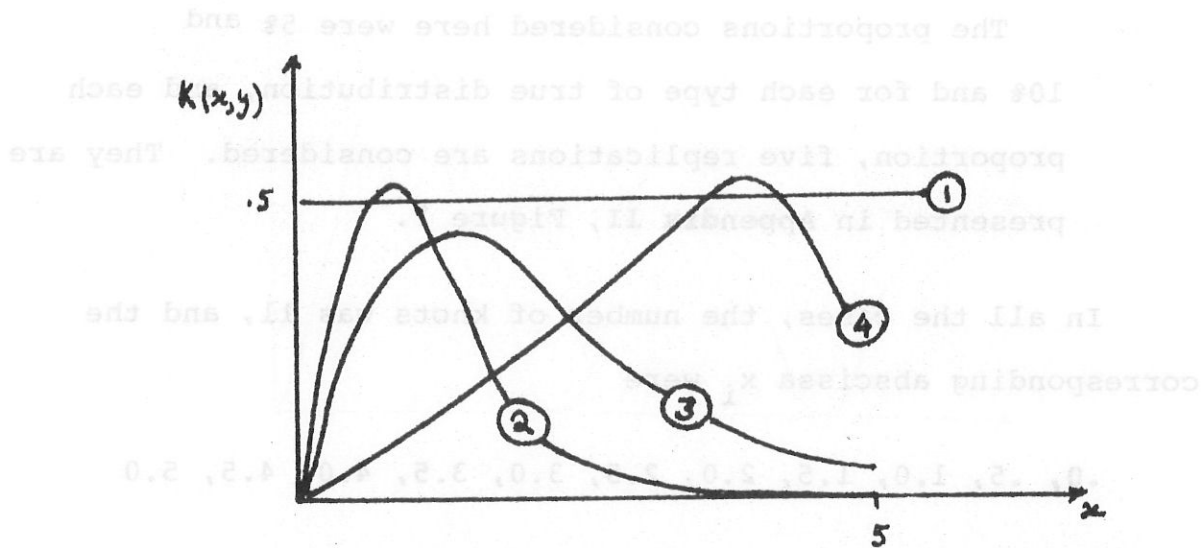


Figure 2.d. The four first approximations.

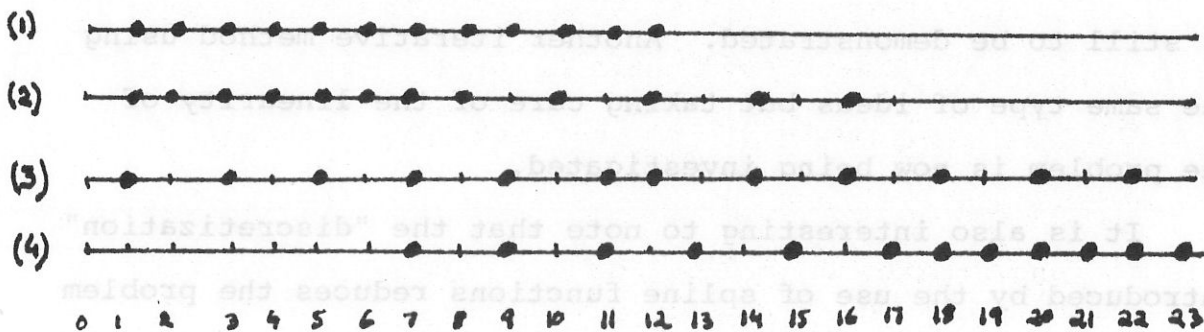


Figure 2.e. The four sets of angles (in degrees).

The proportions considered here were 5% and 10% and for each type of true distribution, and each proportion, five replications are considered. They are presented in Appendix II, Figure 7.

In all the cases, the number of knots was 11, and the corresponding abscissa x_i were

.0, .5, 1.0, 1.5, 2.0, 2.5, 3.0, 3.5, 4.0, 4.5, 5.0

In all the cases, $n=12$ measurements were considered, and the approximate solution shown on the graph is the 18th iteration.

An outline of the program is given in Annex II.

VII. Conclusions.

The set of results of Appendix II seems to favor the apriori belief that the method does converge--but the proof, if any, is still to be demonstrated. Another iterative method using the same type of ideas but taking care of the linearity of the problem is now being investigated.

It is also interesting to note that the "discretization" introduced by the use of spline functions reduces the problem (1) to the solution of an (ill-conditioned) linear system

$$U = Xa \quad (33)$$

where $U \in R^n$

$$X = (X)_{ij_\alpha} : R^{4m} \rightarrow R^n$$

$$a \in R^{4m}$$

$$\text{with } (x_{ij\alpha}) = \int_{x_{j-1}}^{x_j} K(x, y_i) x^\alpha dx \quad (34)$$

$$i=1, \dots, n$$

$$j=1, \dots, m$$

$$\alpha=0, \dots, 3$$

$$\text{and } j_a = 4(j-1) + \alpha \quad (35)$$

a being the vector of coefficients $a_{\alpha j}$ of equation (17) satisfying the conditions S_2 and S_3 of page 6. Using the explicit form of S_2 and S_3 , it is easy to prove that this leads to a system of $m+1$ equations with $m+1$ unknowns, namely the values of $f^0(x)$ at the knots!

The empirical study which results are presented here leads to the following conclusions:

- * The main role of the first approximation $f^1(x)$ is to introduce in the solution the behaviors that the kernel functions are unable to detect (here, the behavior of the true distribution in the neighborhood of the origin--see the results with the first approximation (1)). Except for that fact, the solution is not very sensitive to the exact form of the first approximation, as long as this first approximation is not too oscillating.
- * As mentioned earlier, the influence of the angles of observation is more difficult to summarize: there is clearly a problem of "optimal" set for a given number of angles, since the kernel functions are absolutely not orthogonal in this case.

- * There seems to be no substantial loss of accuracy due to the use of the spline approximation, since the number $m+1$ of knots can be chosen large enough without any difficulty, to give a good representation of the unknown $f^0(x)$ as well as the kernels $K(x, y_i)$.
- * The effect of noise seems to limit the use of the algorithm to accurate measurements (noise $\leq 5\%$) but it is to be noted that only 12 measurements were considered here; in the case of a Type II curve, this seems to be a small number and, even in this case, the precision can be increased by taking multiple measurements for the same angle and considering the mean so that, when multiple measurements are possible, this is not a too serious limitation.

But another interesting point shown by the graphs of Appendix II, Figure 7, is the "unstability" of the problem, or the algorithm, or both: a relatively small change in the μ_i^0 induces an important variation of the "solutions", i.e., of the functions giving almost the same measurements μ_i^N when observed through the filter

$$\int K(x, y_i) f^N(x) dx \quad (36)$$

REFERENCES

- [1] M. T. Chahine. Determination of the temperature profile in an atmosphere from its outgoing radiance, J. Opt. Soc. Am. 58, 1634-1637, 1968.
- [2] W. L. Smith. Iterative solution of the radiative transfer equation for the temperature and absorbing gas profile of an atmosphere, Applied Optics 9, September 1970.
- [3] I. J. Schoenberg. Contribution to the problem of approximation of equidistant data by analytic functions, Quarterly of App. Math. 4, 1946.
- [4] T. N. E. Greville. Spline functions and applications, M.R.C., University of Wisconsin, Orientation Lecture Series No. 8.
- [5] K. S. Shifrin. Scattering of light in a turbid medium, NASA TT-F477, NASA, Washington, D.C., 212-1968.
- [6] K. S. Shifrin and E. A. Chayanova. The determination of the vertical spectrum from the scattering formula, Izv. Atm. & Oceanic Phys. 2, 2, 1966.

Appendix I.

Atmospheric physicists have exhibited considerable interest in determining size distributions of aerosols. Although aerosol particles may be collected and measured individually, this is a tedious task which can be avoided by employing optical scattering measurements.

It is feasible to measure light scattered forward by relatively small angles θ to derive information on aerosol size distributions. The phase function can be derived rigorously from Mie theory, however the computation is time consuming. We therefore employed an approximation to the Mie scattering kernel $i(\theta, r)$ due to Shifrin [5] which is valid for "soft" particles, namely those with

$$\frac{2\pi r_0}{\lambda} (m-1) < 1 \quad \text{and} \quad \frac{3}{4\pi} \left(\frac{m^2-1}{m^2+1} \right) < 1$$

m : refractive index of the material of which the spheres are composed.

r_0 : characteristic particle radius

λ : wave length of the incident light

The phase function is

$$P(\theta) = \text{const.} \int_0^\infty i(\theta, r) \eta(r) dr \quad (\text{A.1})$$

this integral equation was transformed by Shifrin and Chayanova [6] into

$$\mu(y) = \int_0^\infty K(x, y) f(x) dx \quad (\text{A.2})$$

$$f(x) = r_0^4 x^2 \eta(x) \quad (A.3)$$

$$K(x,y) = (\cos xy - \frac{1}{xy} \sin xy)^2 \quad (A.4)$$

$$y = \frac{4\pi r_0}{\lambda} \sin \frac{\theta}{2} \quad (A.5)$$

$$x = r/r_0 \quad (A.6)$$

the computations were conducted for

$$m = 1.1 \quad r_0 = \lambda = .5\mu$$

A beam of light entering a turbid medium consisting of spherical aerosols is extinguished in accord with Bear's law. The extinction coefficient, K , is a function of the size distribution of the aerosols, $\eta(r)$

$$K = \int_0^{\infty} Q\pi r^2 \eta(r) dr \quad (A.7)$$

where Q is the ratio between the optical scattering cross-section and the geometric cross-section of the aerosol particles. This quantity can be derived by Mie theory, but we will employ an approximation which is valid for $|m-1| < 1$ in order to facilitate the numerical analysis

$$Q \approx 2 - \frac{4}{\rho} \sin \rho + \frac{4}{\rho^2} (1 - \cos \rho) \quad (A.8)$$

where

$$\rho = \left[\frac{4\pi r_0}{\lambda} (m-1) \right] x \quad (A.9)$$

Although the extinction coefficient was initially used to derive the aerosol size distribution, it contributed little information in comparison with the phase function computations. The results shown here were therefore computed without recourse to it.

Appendix II.

A. Influence of variation of the first approximation $f^1(x)$:

Table 1-2: value of observed μ_i^0 and approximated μ_i^{18} ($i=1, \dots, 12$) for the four different $f^1(x)$.

Figure 3-4: True and approximate solutions.

B. Influence of variation of the angles.

Figure 5-6: True and approximate solutions.

C. Influence of errors.

Figure 7: True solution and variation of the approximation.

D. Influence of an acceleration parameter (Figure 8).

		μ_i^{18}				
Angle	$\tilde{\mu}_i^0$	(1)	(2)	(3)	(4)	i
1	.00	.00	.00	.00	.00	1
2	.00	.00	.00	.00	.00	2
4	.01	.02	.02	.02	.02	3
6	.06	.06	.06	.06	.06	4
8	.12	.12	.12	.12	.12	5
10	.19	.19	.19	.19	.19	6
12	.25	.25	.25	.25	.25	7
14	.28	.29	.29	.30	.29	8
16	.30	.31	.31	.32	.30	9
18	.31	.31	.31	.32	.30	10
20	.30	.30	.30	.29	.29	11
22	.29	.29	.28	.27	.29	12

For Type I, and

$$\tilde{\mu}_i^{18}$$

Angle	$\tilde{\mu}_i^0$	(1)	(2)	(3)	(4)	i
1	.00	.00	.00	.00	.00	1
2	.03	.03	.03	.03	.03	2
4	.30	.31	.31	.31	.30	3
6	.70	.68	.67	.67	.68	4
8	.74	.66	.65	.66	.70	5
10	.54	.53	.52	.53	.56	6
12	.55	.62	.62	.62	.63	7
14	.67	.71	.71	.72	.73	8
16	.69	.68	.68	.69	.72	9
18	.68	.67	.67	.68	.69	10
20	.67	.66	.67	.66	.53	11
22	.65	.66	.66	.64	.58	12

for Type II.

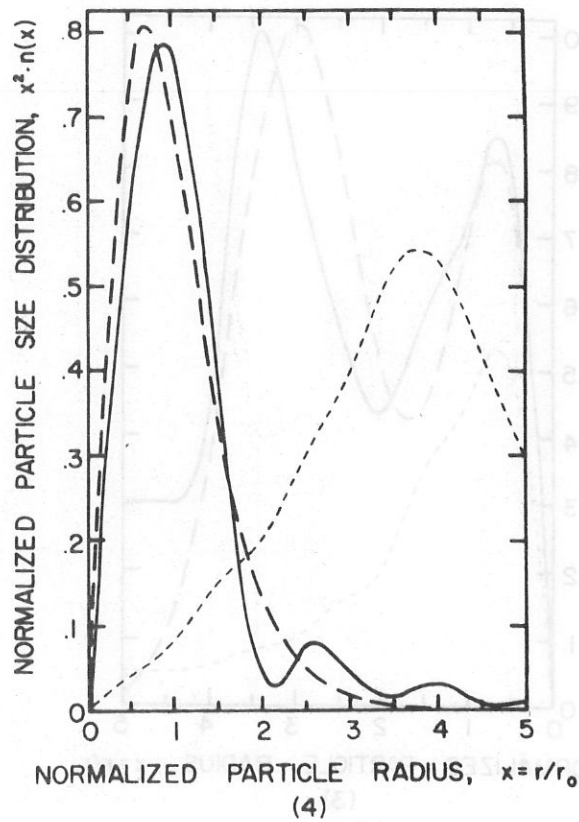
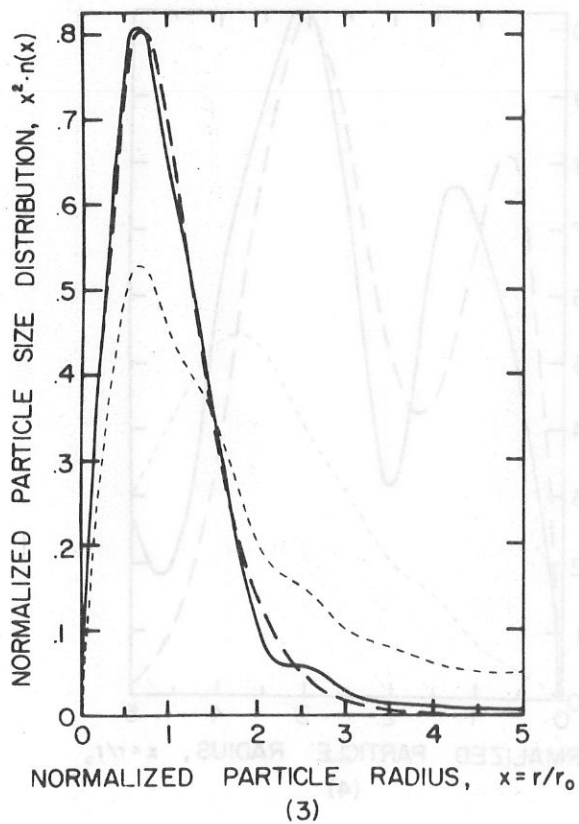
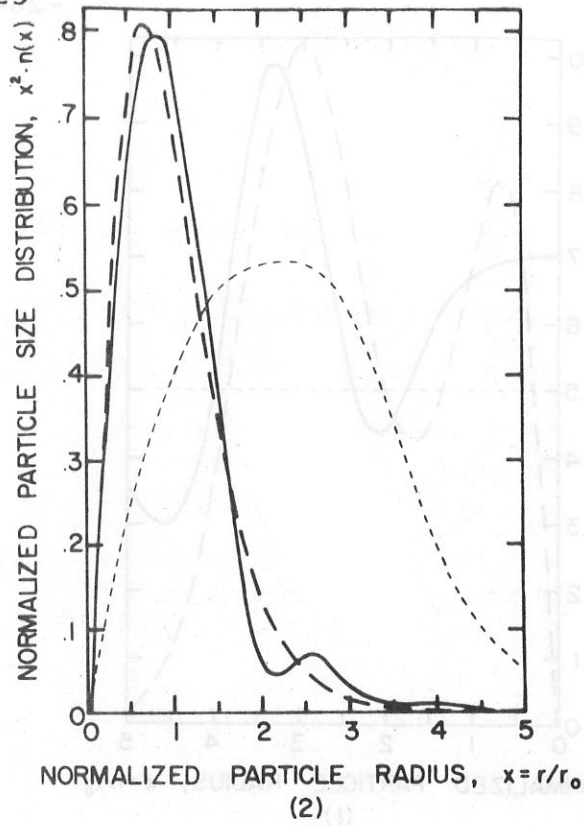
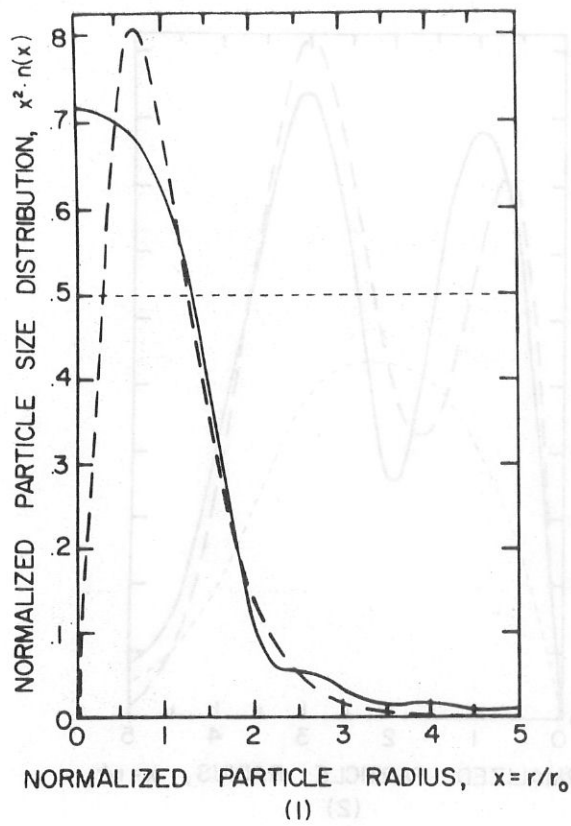


Figure 3. Effect of various initial trial solutions on iterated unimodal solution of Fredholm integral equation. Trial solution, -----. True solution, ---. Iterated solution, —.

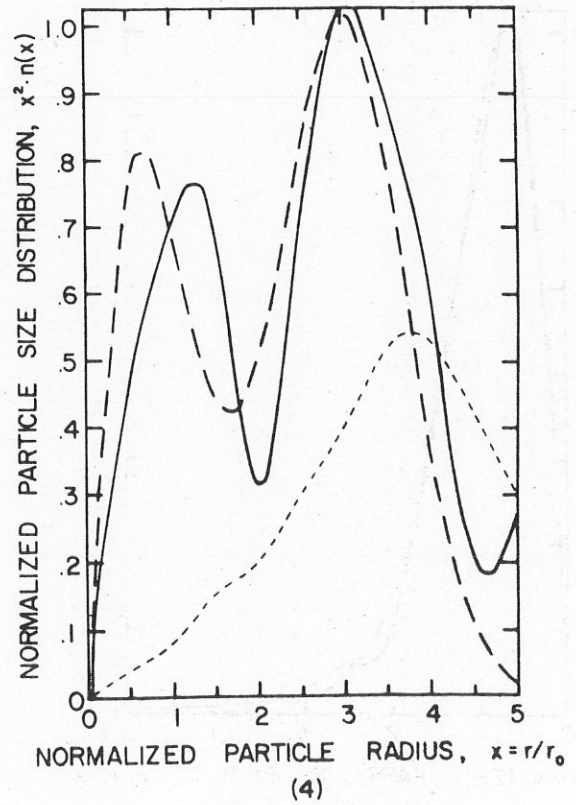
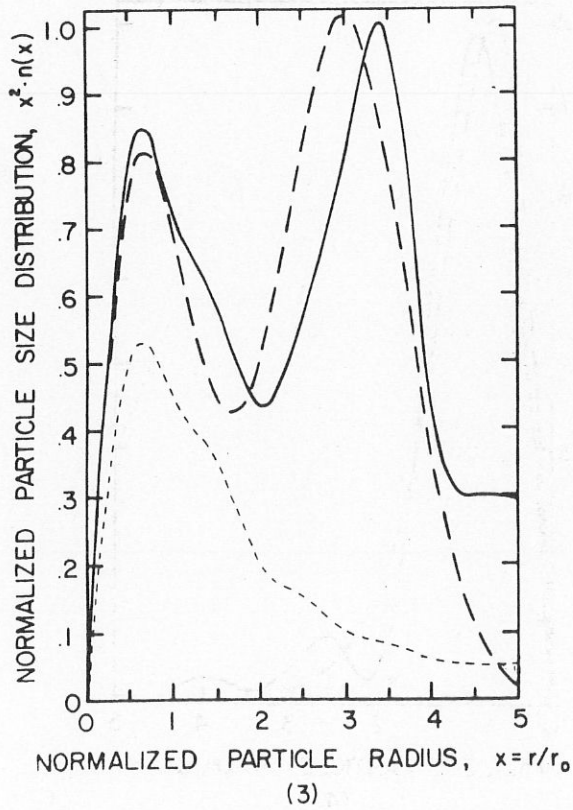
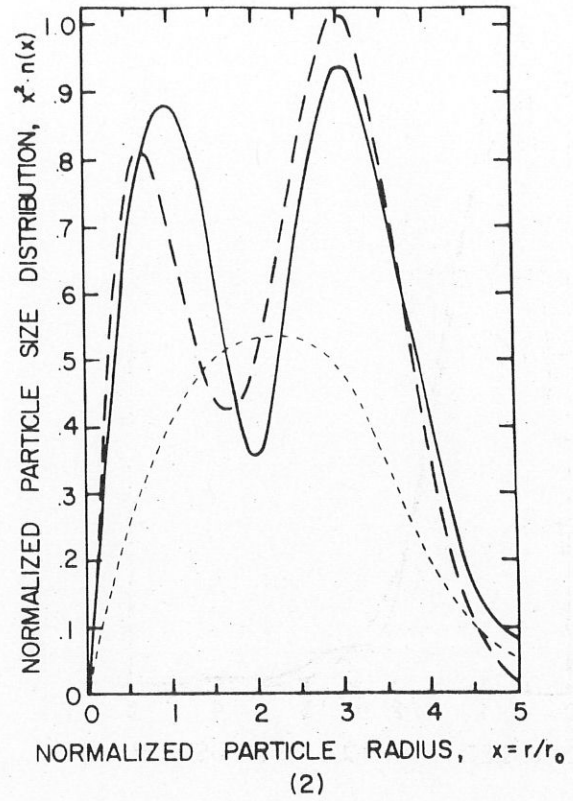
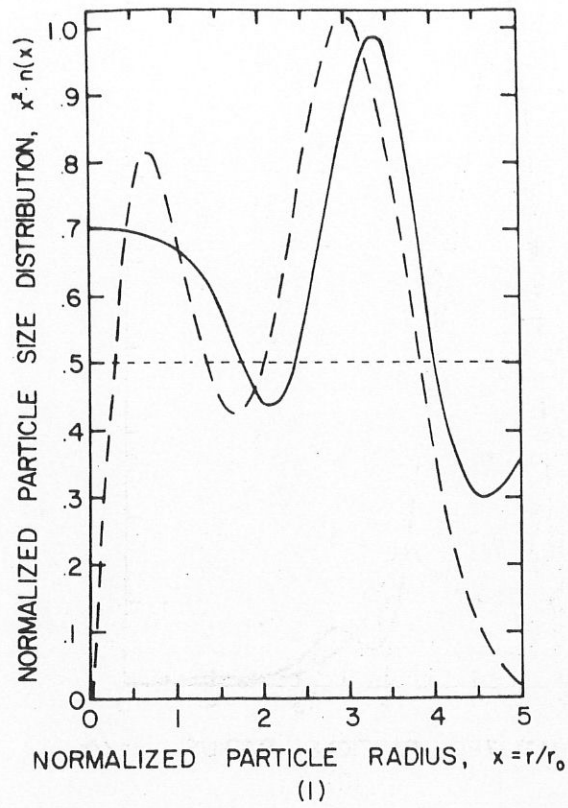


Figure 4. Effect of various initial trial solutions on iterated bimodal solution of Fredholm integral equation. Trial solution, ----. True solution, - - -. Iterated solution, —.

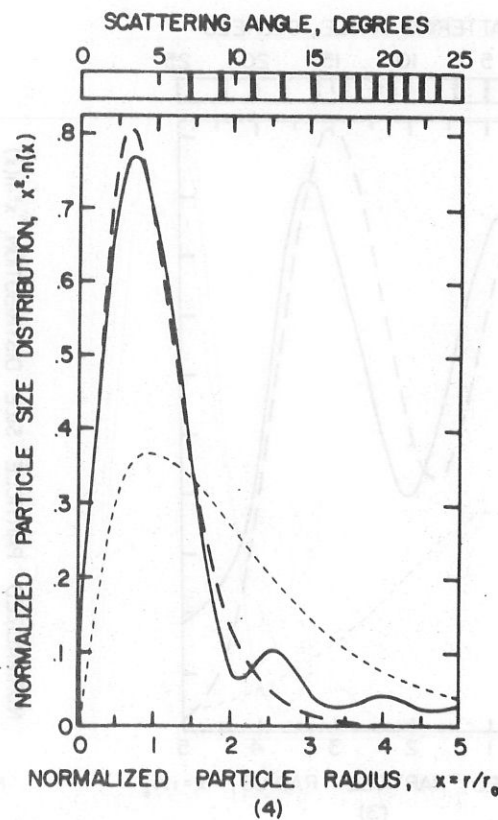
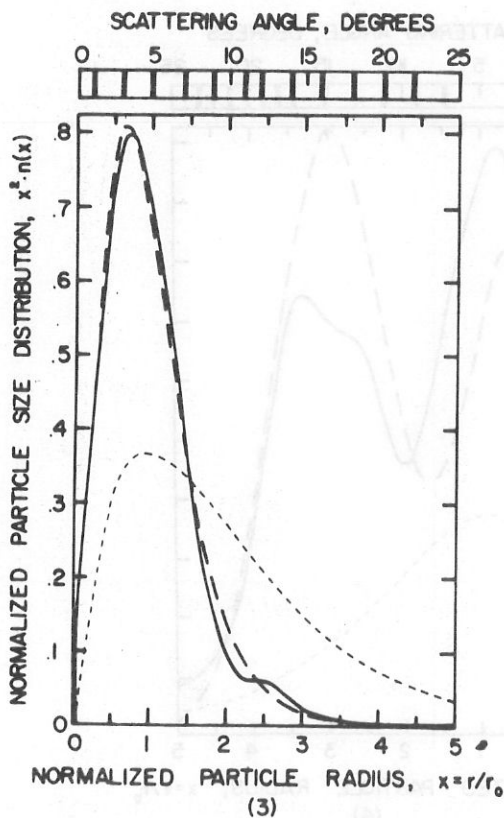
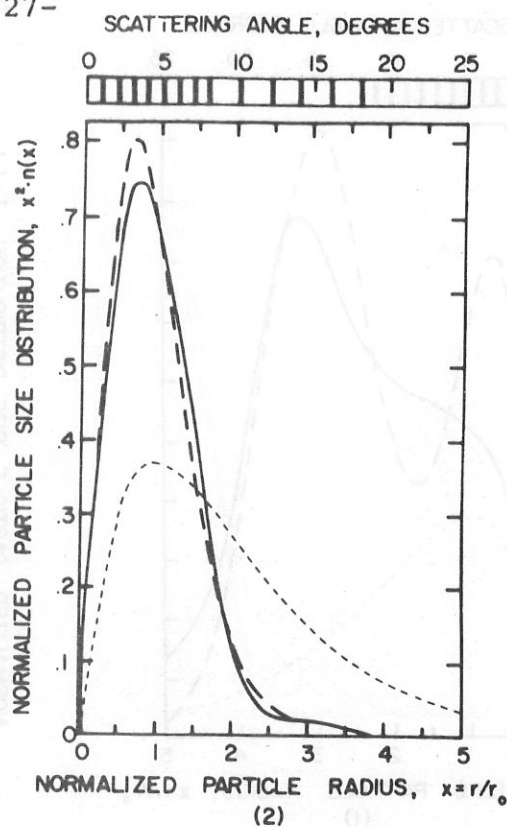
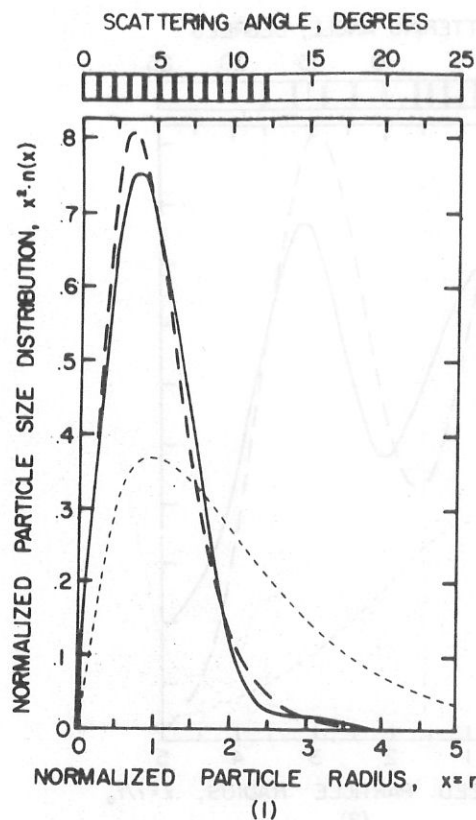


Figure 5. Effect of varying scattering angles at which the phase function is measured on a unimodal size distribution. Trial solution, - - - - - . True solution, — — — . Iterated solution, — · — · — · . (Twelve "measured" scattering angles are shown above each figure.)

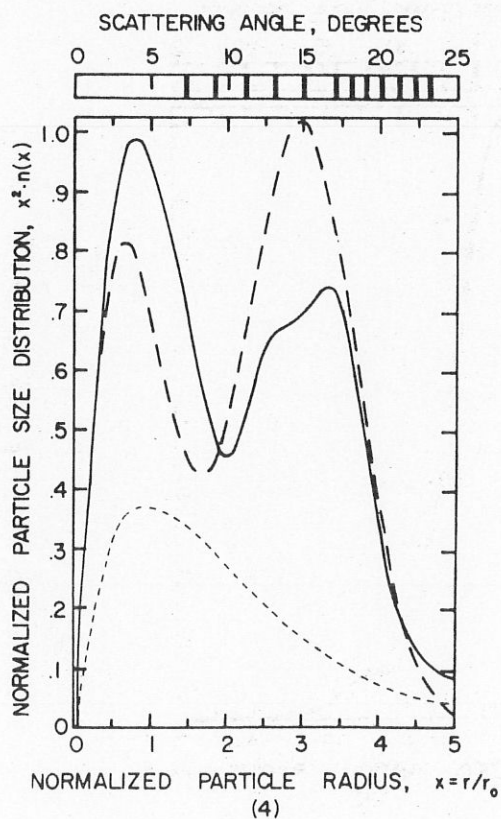
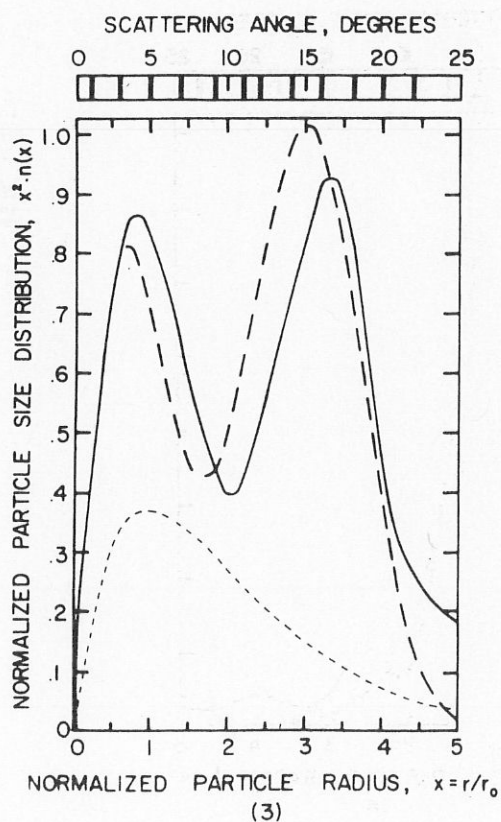
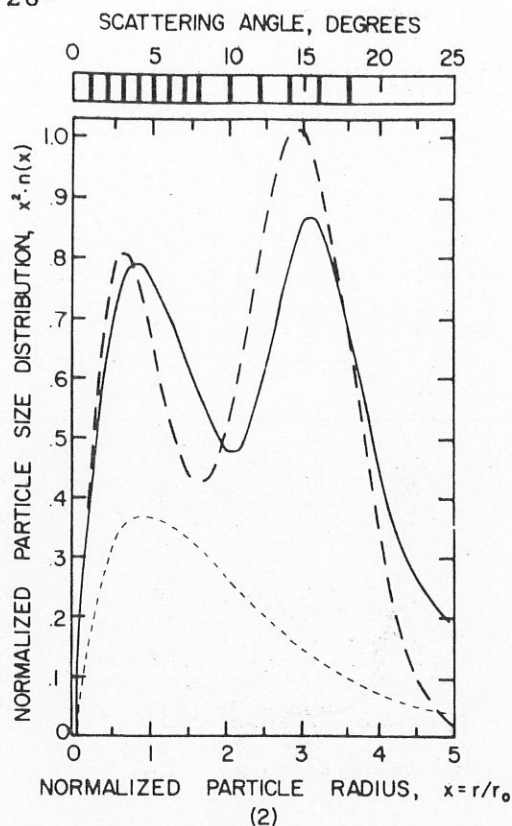
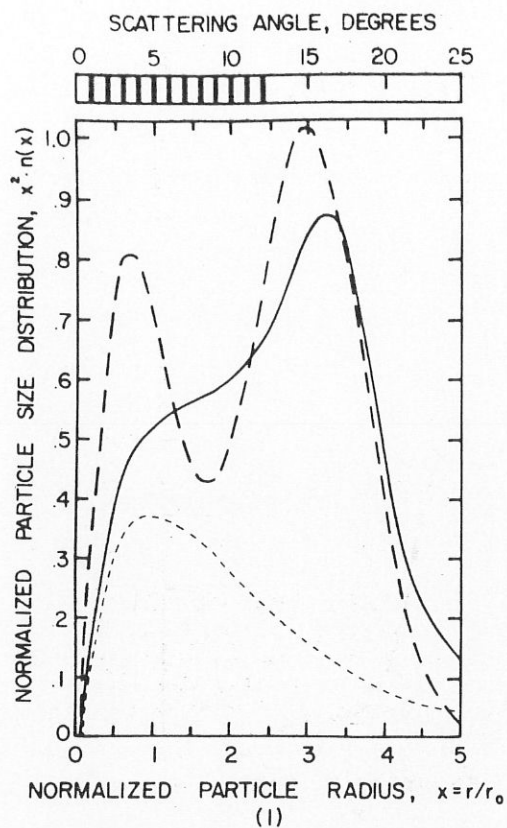


Figure 6. Effect of varying scattering angles at which the phase function is measured on a bimodal distribution. Trial solution, ----. True solution, ——. Iterated solution, ———. (Twelve "measured" scattering angles are shown above each figure.)

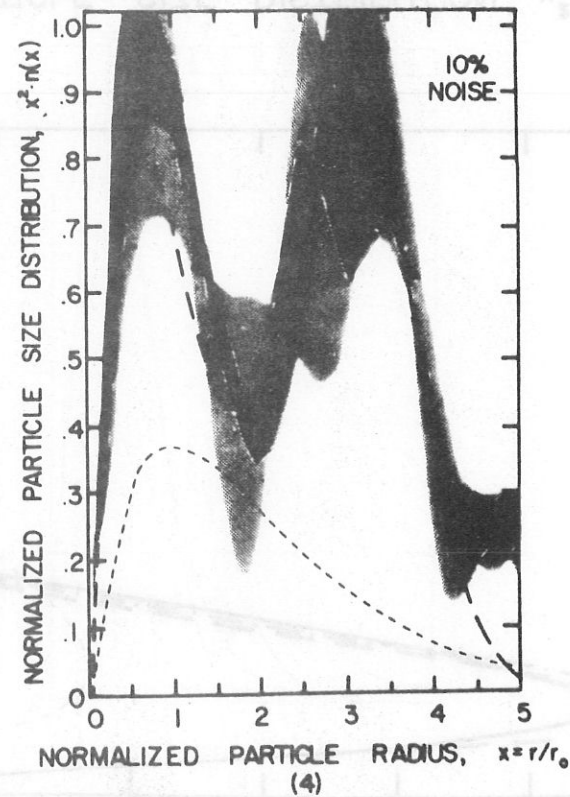
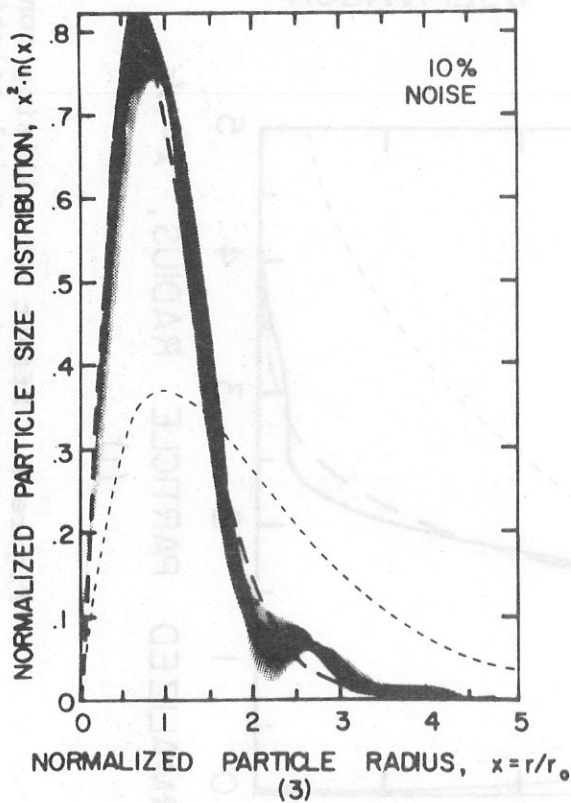
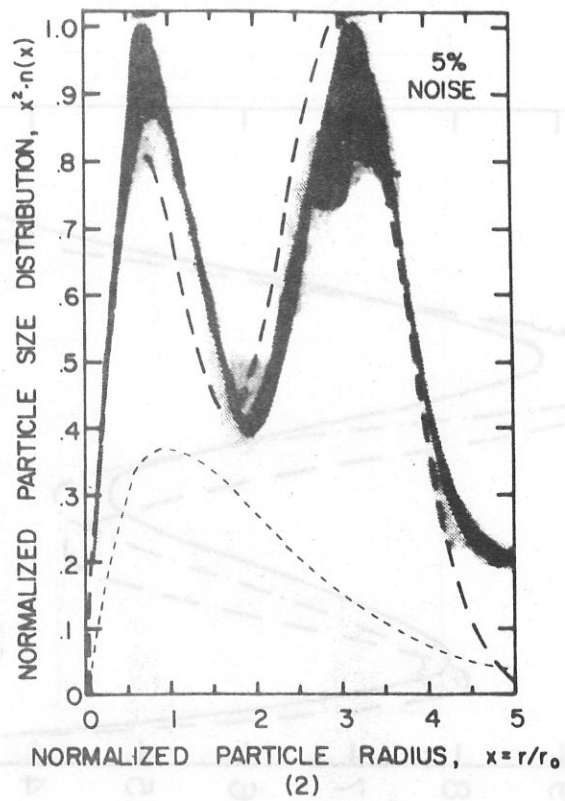
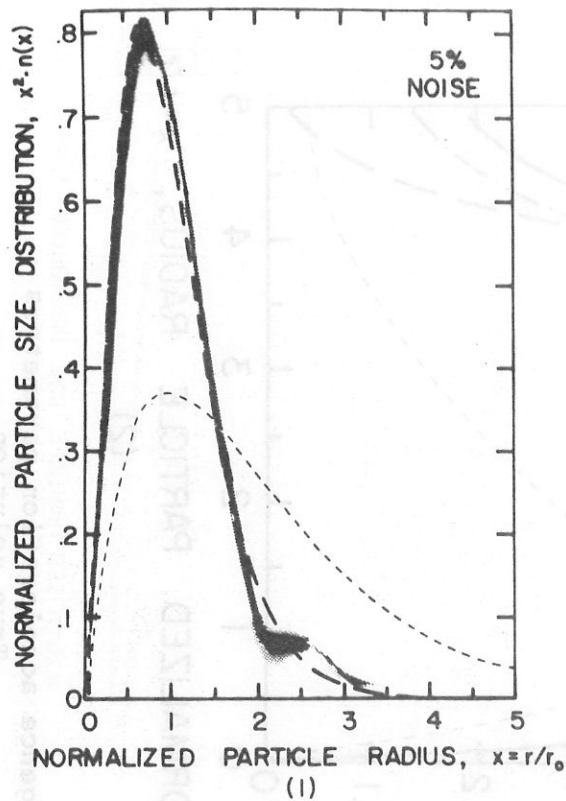


Figure 7. Effect of noise on iterated solutions of Fredholm integral equations. Most probable solution (60% of cases), dark shading. Less probable solution (40% of cases), light shading. Trial solution, ----. True solution, — — —.

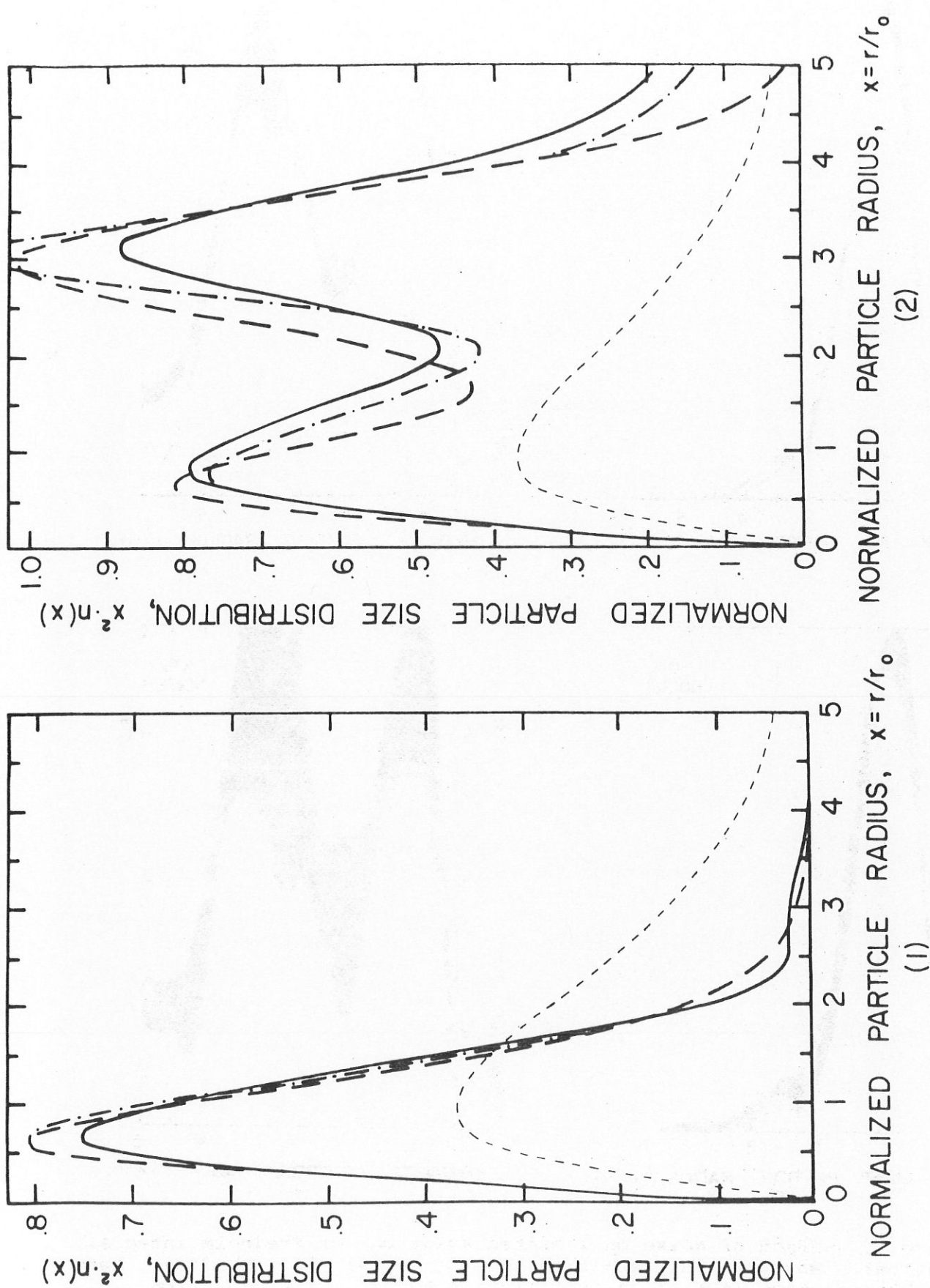


Figure 3. Effect of utilizing convergence acceleration parameters after 12 iterations. Trial solution, ---. True solution, —. Chahine and Smith solution without accelerating parameter, ---. Solution with accelerating parameter, —.

Appendix III. Outline of the program.

There is no major difficulty in the program, as soon as good subroutines for computation of the spline coefficients and for integration are available.

Are to be chosen:

- the knots x_0, \dots, x_m
- the angles of interest y_1, \dots, y_n
- the values of the true distribution $f(x_0), \dots, f(x_m)$
- the values of the first approximation $f^1(x_0), \dots, f^1(x_m)$
- the number of iteration.

Then:

1. The quantities

$$\int_{x_{i-1}}^{x_i} K(x, y_j) (x - x_{i-1})^a dx$$

or

$$\int_{x_{i-1}}^{x_i} K(x, y_j) (x)^a dx$$

(depending on which of the equations (17) or (17') will be used by the spline subroutine to give the spline approximation)

are computed for $i=1, \dots, m$

$j=1, \dots, n$

$a=0, \dots, 3$

and stored in a (tri-dimensional) array.

2. The values of the weights

$$\frac{K(x_i, y_j)}{\sum_{j=1}^n K(x_i, y_j)}$$

are derived and stored in two-dimensional array.

3. Using the spline subroutine and formula (21) first with the $(x_i, f^0(x_i))$, then with the $(x_i, f^1(x_i))$ the quantities μ_j^0 and μ_j^1 are derived for $j=1, \dots, n$.

4. The $f^2(x_i)$ ($i=0, \dots, m$) are derived using (22). Using the spline subroutine and (20) with $(x_i, f^2(x_i))$, the quantities μ_j^2 ($j=1, \dots, n$) are derived, and the program goes back to 4 with $N+1$ instead of N as many times as the chosen number of iterations.